Fatigue Behaviour of Laserbeam Welded Thin Steel and Aluminium Sheets under Multiaxial Loading

J. Wiebesiek, K. Störzel, T. Bruder, H. Kaufmann

Fraunhofer Institute for Structural Durability and System Reliability LBF, Darmstadt / Germany, E-mail: jens.wiebesiek@lbf.fraunhofer.de

ABSTRACT. *Laserbeam welded tubular specimens with overlap joints made from structural steel St35 (S235 G2T), artificially hardened aluminium alloy AlSi1MgMn T6 (EN AW 6082 T6) and self-hardening aluminium alloy AlMg3.5Mn (EN AW 5042) were investigated under proportional and non-proportional multiaxial loading with constant amplitudes in the range of $2 \cdot 10^4$ to $1 \cdot 10^7$ cycles. The multiaxial fatigue behaviour of these joints was assessed by the concept of the reference radius r_{ref} = 0.05 mm. The equivalent stresses, especially considering the fatigue life reducing influence in case of non-proportional loading in comparison to proportional loading, were calculated by the Effective Equivalent Stress Hypothesis (EESH) and with a recently developed hypothesis which is called Stress Space Curve Hypothesis (SSCH). This hypothesis is based on the time evolution of the stress state during one load cycle.*

INTRODUCTION

In automotive, aerospace and chassis structures the joining technology of laserbeam welding is widely used. This technology enables to join effectively thin and filigree components for lightweight structures with sufficient stiffness.

The fatigue behaviour of these structures is influenced by many factors. Beside the geometry of the weld, possible crack like defects and/or gas pores and the presence of residual stresses, the complex stress state in the fatigue critical area is a very important factor. In general, the stress state is not constant during the load-time history. Principal stress directions can change, for instance when non-proportional multiaxial loads occur. The influence of changing principal stress directions on fatigue life depends on the materials ductility and on the elongation. In case of rotating principal stress directions ductile materials react with lifetime shortening compared to constant principal stress directions. For a semi-ductile material state the fatigue behaviour related to constant or changing principle stress directions is indifferent. In comparison to ductile materials under non-proportional loading the lifetime of brittle (low-ductile) materials is increased.

In the present paper the influence of changing principal stress directions on fatigue life of laserbeam welded overlapped tube-tube specimens is addressed. It is discussed if conventional strength hypotheses, like von Mises, are able to describe the present

fatigue behaviour sufficiently under such complex loading. Further on, a recently developed equivalent stress hypothesis [1, 2] is presented by considering effects which can occur under multiaxial loading. The fatigue results are additionally evaluated with the hypothesis EESH [3].

SPECIMENS, MATERIAL AND TESTING

Material

Laserbeam welded tube-tube specimens of three different materials were examined in this investigation. Base material of the specimens were extruded aluminium tubes of the self hardening alloy AlMg3.5Mn (EN AW 5042) the artificially hardened alloy AlSi1MgMn T6 (EN AW 6082 T6) and seamless tubes of the structural steel St35 (S235 G2T).

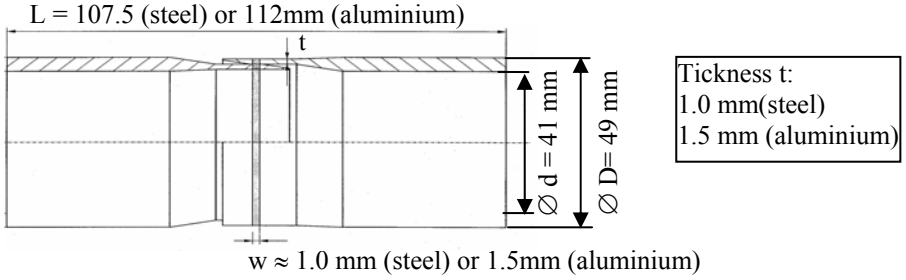

Figure 1. Laser beam welded, overlapped tube-tube specimen

	$R_{p0.2}$ [MPa]	R_m [MPa]	E [GPa]	e [%]	ν	HV0.1
St35	235	405	210	26	0.30	203
AlMg3.5Mn	127	269	71	20	0.33	98
AlSi1MgMn T6	341	359	71	17	0.33	115

Table 1. Conventional mechanical properties of the specimens

Testing

The tube-tube specimens were tested in a servo-hydraulic biaxial test rig with a 100 kN axial and a 3.0 kNm torsion actuator under load control with a testing frequency of 20 Hz. The load ratio was R = -1. Failure criterion was the total failure / rupture of the specimens. All tests were carried out under laboratory conditions in air at room temperature. Fatigue test results for constant amplitudes of pure axial loading, pure torsion, combined axial and torsion in-phase (φ=0°) and combined axial and torsion out-of-phase (φ=90°) loading for each material are presented. The selected ratio of the nominal shear to the nominal normal stress amplitudes of the combined loading was τ_{na}/σ_{na} = 1.3 respectively 28 Nm/kN. This ratio was chosen in a way that the equivalent von Mises stresses in the notch root were equal for each loading component, i.e. $\tau_{v.Mises,local}$ / $\sigma_{v.Mises,\ local}$ = 1.0.

EXPERIMENTAL RESULTS AND EVALUATION

The experimental results and the obtained SN curves for 50% probability of survival are given in Figs. 2 to 4. The cracks started in the weld roots between the tube halves and propagated through the heat affected zone of the outer tube walls. The experiments with steel joints reveal a significant difference between in- and out-of-phase combined loadings. Out-of-phase loading reduces the fatigue life compared to in-phase loading, Fig. 2. This fatigue behaviour was already observed in earlier investigations [4]. An important result is that for the investigated aluminium alloys the fatigue life is also reduced in case of out-of-phase loading in a range between 10^4 and $2 \cdot 10^5$ cycles, Figs. 3 and 4.

The local stresses in the fatigue critical area were calculated for pure axial and pure torsional load by linear-elastic FEM calculations. This was done by modelling the weld roots by a keyhole notch with a fictitious radius of r_{ref} = 0.05 mm [4]. This local reference radius concept has already been used successfully for the assessment of welded structures from thin sheets with sharp weld roots [5, 6] and is today a standard method in the German automotive industry.

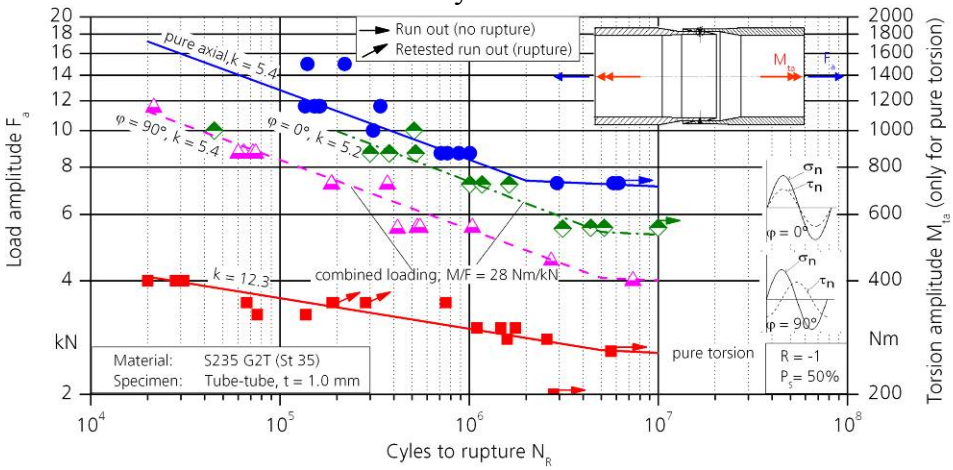

Figure 2. Experimental results for the structural steel S235

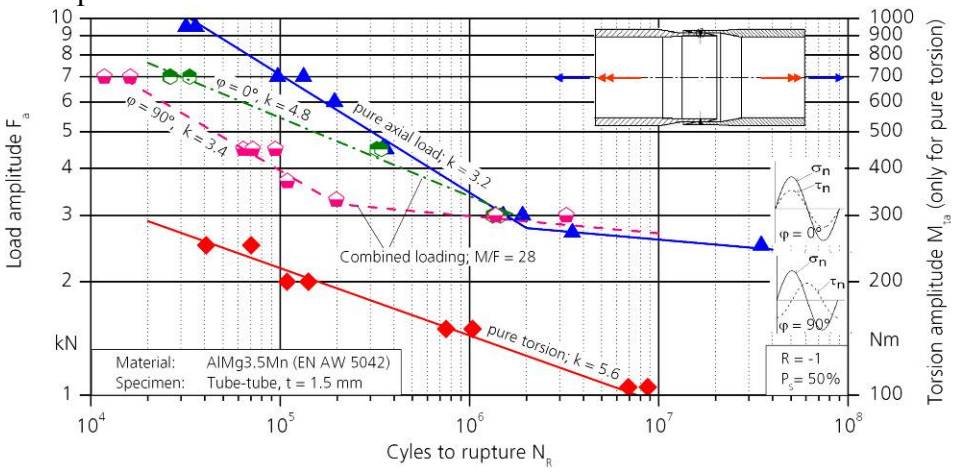

Figure 3. Experimental results for the self hardening aluminium alloy AlMg3.5Mn

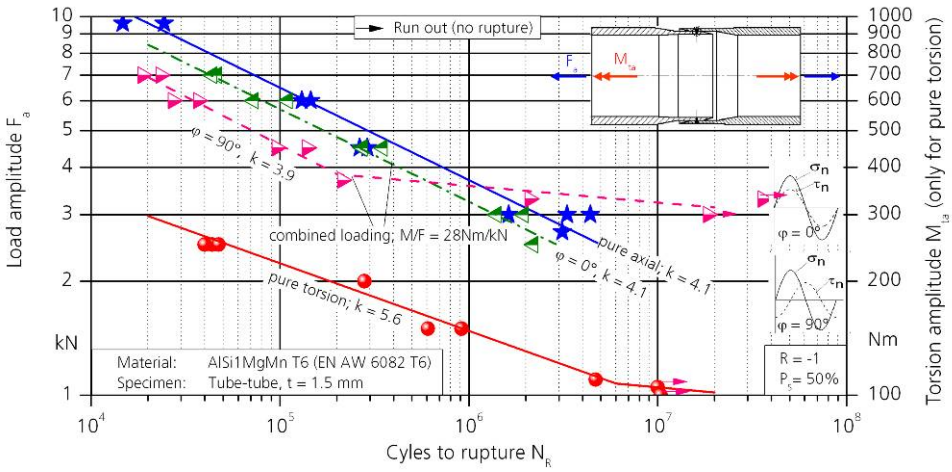

Figure 4. Exp. results for the artificially hardened aluminium alloy AlSi1MgMn T6

ASSESSMENT OF LOCAL MULIAXIAL STRESSES

The aim is to calculate the lifetime, respectively the corresponding equivalent stresses for complex multiaxial loadings. Both hypotheses SSCH and EESH use the local stress SN curves for pure axial and pure torsion loadings (local stress components calculated by FEM) as input values.

The **S**tress **S**pace **C**urve **H**ypothesis equivalent stress does not fit in the classification that groups multiaxial fatigue criteria into critical plane or integral stress approaches. Both of these groups take time-independent values as input variables, for instance a maximum (taken from all possible planes and from one cycle) of a certain stress variable that is considered to be the damage-relevant variable, or an integral value of such stress variable (integrated over all possible planes over one cycle). The basic idea of the SSCH is to take into account the complete time evolution of the (multidimensional) stress signal. The approach of the current version of the SSCH can be subdivided into three parts:

a) Generalization of approaches that have a form similar to von Mises or Tresca:

In the current version of the SSCH the stress signal is viewed at in a three-dimensional space p-q-τ, which is defined as:

$$p(t) = 0{,}5 \cdot (\sigma_x(t) + \sigma_y(t)) \; ; \; q(t) = 0{,}5 \cdot (\sigma_x(t) - \sigma_y(t)) \; ; \; \tau(t) = \tau_{xy}(t) \qquad (1)$$

These stress coordinates refer to the Mohr's circle for a plane stress state. The p-q-τ-space signals for proportional loadings result in line segments. The basic idea is that the length of such stress space line segment is the damage-relevant variable. This means, that different types of uniaxial loadings with the same lifetime should lead to line segments with the same length. To fulfil this condition, the stress variables p, q and τ are multiplicated with weighting factors

$$p \rightarrow \cdot\sqrt{\alpha} \; ; \; q \rightarrow \cdot\sqrt{4-\alpha} \; ; \; \tau \rightarrow \cdot\sqrt{4-\alpha} \quad . \qquad (2)$$

This rescales the p-q-τ-space into a new stress space. The assumption in the basic version of SSCH is that the damage of proportional loadings is proportional to the half-length of the line segment in the rescaled space and this length is taken as an equivalent stress:

$$\sigma_{eq,SSCH} = \sqrt{\alpha p_a^{\,2} + (4-\alpha) q_a^{\,2} + (4-\alpha)\tau_a^{\,2}} = \sqrt{\alpha p_a^{\,2} + (4-\alpha)\left(q_a^{\,2} + \tau_a^{\,2}\right)} \qquad (3)$$

This approach can be linked to other hypotheses like the von Mises (α=1) or the Tresca-Criterion (α=0). For this basic version of SSCH, part of the task is to find the correct scaling factor alpha for certain specimens, which may depend on material and/or geometry. The p-q-τ-space signals for constant amplitude out of phase loadings, yet with the same frequency, result in ellipses in the p-q-τ-space, Fig. 5. The shapes of the ellipses are invariant against a rotation of the coordinate system. In first order, the damage of the ellipse is considered to be proportional to the half-length of the diagonal of the circumscribing rectangle, covering the half-length of the proportional loading line-segment as a special case (equation (3)).

b) The second part of the SSCH approach is a consideration of out-of phase effects:
To cover different kinds of out of phase effects, an additional factor is added to (3):

$$\sigma_{eq,SSCH} = \sqrt{\alpha p_a^{\,2} + (4-\alpha)\left(q_a^{\,2} + \tau_a^{\,2}\right)} \cdot \left(1 + \frac{\rho \cdot a \cdot b}{a^2 + b^2}\right) \qquad (4)$$

The additional factor depends on the ratio of the ellipses semi-minor axis a to its semi-major axis b, ρ is an additional parameter that may depend on the specimen's material and/or its geometry.

The reason of this approach is that increasing the phase difference φ_{xy} for the same loading amplitudes leads to a growing ellipse that is still located in the same rectangle, Fig. 5.

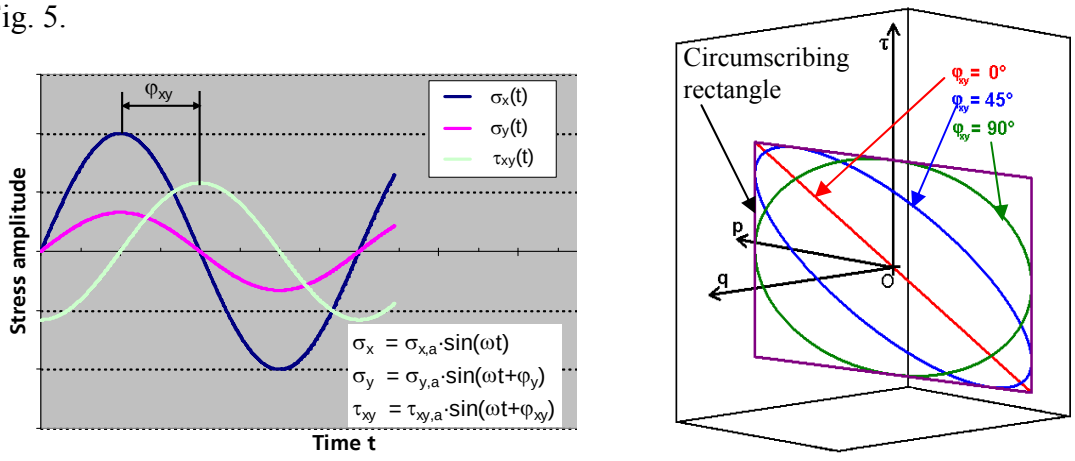

Figure 5. Stress space curves for different combined load cases (φ_{xy} = 0°, 45° and 90°)

Depending on the sign of ρ, it is possible to cover all three kinds of out of phase effects (lifetime shortening, lifetime lengthening or neutral behaviour).

c) The third part of the SSCH approach takes into account, that the slopes of the basic SN curves may be different:
Comparing the basic SN curves for pure axial and pure torsion loading with the previous SSCH formula leads to a proportional coherency between these two types of loadings (assumption: $\sigma_y = \nu \cdot \sigma_x$; for plane stress state at the surface in the notch):

$$\sigma_{eq,SSCH,Axial} = \sigma_{x,a}\sqrt{1+\nu^2+(\alpha-2)\nu}\;;\; \sigma_{eq,SSCH,Torsion} = \tau_{xy,a}\sqrt{(4-\alpha)} \tag{5}$$

This would lead to a torsion SN curve being parallel to the axial SN curve. But in general the slopes of these two lines are not equal (and in most cases they are unequal). To cover this fact, the previous SSCH formula is modified. The constant α is now considered to depend on the lifetime N: $\alpha = \alpha(N)$. (This approach takes also in account that fatigue processes may be based on different damage mechanisms). The function $\alpha = \alpha(N)$ can be calculated by comparing points on the axial and torsional SN curves that belong to the same lifetime N:

$$\sigma_{eq,SSCH,Axial}(N) \overset{!}{=} \sigma_{eq,SSCH,Torsion}(N) \;\Rightarrow\; \alpha(N) = 4 - \frac{(1+\nu)^2}{\nu + \tau_{xy,a}^{\,2}(N)/\sigma_{x,a}^{\,2}(N)} \tag{6}$$

$$\sigma_{eq,SSCH}(N) = \sqrt{\alpha(N)p_a^{\,2} + (4-\alpha(N))\left(q_a^{\,2}+\tau_a^{\,2}\right)}\cdot f_\rho\left(a/b\right), \tag{7}$$

Formula 7 shows the whole SSCH that is currently used, which must be solved numerically in a way that the point $(\sigma_{eq,SSCH}(N);N)$ fits onto a reference SN curve.

The **E**ffective **E**quivalent **S**tress **H**ypothesis method belongs to the group of integral stress approaches, valid for ductile materials. In case of proportional loadings the EESH equivalent stress is the von Mises approach.

$$\sigma_{eq,Mises} = \sqrt{\sigma_{x,a}^2 + \sigma_{y,a}^2 - \sigma_{x,a}\sigma_{y,a} + 3\tau_{xy,a}^2} \tag{8}$$

Taking into account that the basic SN curves for pure axial and pure torsional loading often have different slopes and different position, a size factor f_G is added to the torsional component:

$$\sigma_{eq,EESH} = \sqrt{\sigma_{x,a}^2 + \sigma_{y,a}^2 - \sigma_{x,a}\sigma_{y,a} + 3\tau_{xy,a}^2 \cdot \underbrace{\left(\sigma_{eq,Mises,axial}\left(N(\tau_{xy,a})\right)/\sqrt{3}\tau_{xy,a}\right)^2}_{f_G}} \tag{9}$$

The multiplication with f_G substitutes the von Mises stress component for pure torsion $\sqrt{3}\tau_{xy,a}$ with a von Mises stress from pure axial $\sigma_{eq,Mises,axial}$ taken from the uniaxial SN-curves for same lifetime $N = N(\tau_{xy,a})$. The most important idea of the EESH is that the

arithmetic average of the shear stress amplitudes $\hat{\tau}_{n,a}$ in all considered planes, which is an integral value, is the damage-relevant variable:

- Considered planes : All planes that are orthogonal to the surface
- $\alpha \rightarrow$ Rotation angle, that represents the considered plane ($\alpha \in [0°; 180°]$)
- Formula for the shear stress amplitude in the plane α:

$$\tau_{n,a}(\alpha) = \sqrt{0{,}25(\sigma_{x,a} - \sigma_{y,a})^2 \sin^2(2\alpha) - 0{,}5(\sigma_{x,a} - \sigma_{y,a})\sin(4\alpha)\tau_{xy,a}\cos(\varphi_{xy}) + \tau_{xy,a}^2 \cos^2(2\alpha)} \qquad (10)$$

- Arithmetic shear amplitude average is calculated: $\tau_{arith} = \frac{1}{\pi}\int_0^{\pi} \tau_{n,a}(\alpha)\, d\alpha$ (11)

In line with the uniaxial case $\sigma_{eq,EESH}(\varphi_{xy}=0)$ (formula (9)), the approach $\sigma_{eq,EESH} \propto \tau_{arith}$ leads to the formula:

$$\sigma_{eq,EESH}(\varphi_{xy} \neq 0) = \sigma_{eq,EESH}(\varphi_{xy} = 0)\frac{\tau_{arith}(\varphi_{xy} \neq 0)}{\tau_{arith}(\varphi_{xy} = 0)} \qquad (12)$$

To cover the influence of stress gradients for rotating principal stress directions, concerning more complex geometrical structures, an additional Factor C, depending on the notch factors K_{ta} and K_{tt}, is added and the whole EESH Formula currently used is:

$$\sigma_{eq,EESH}(\varphi_{xy} \neq 0) = \sigma_{eq,EESH}(\varphi_{xy} = 0)\frac{\tau_{arith}(\varphi_{xy} \neq 0)}{\tau_{arith}(\varphi_{xy} = 0)} \cdot \underbrace{\left(\frac{1+K_{ta}}{1+K_{tt}}\right)^{0{,}5\cdot\left[1-\left(\frac{\varphi_{xy}-0{,}5\pi}{0{,}5\pi}\right)^2\right]}}_{C} \qquad (13)$$

Displayed in Figs. 6 and 7 are the calculated life-times N_{calc} versus the experimental life times N_{exp}.

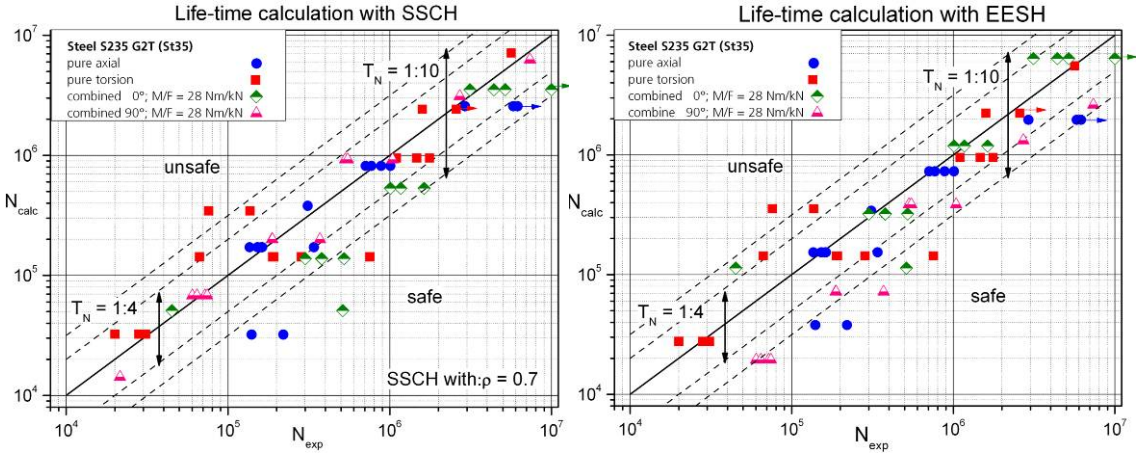

Figure 6. N_{calc} vs. N_{exp} diagrams for steel joints

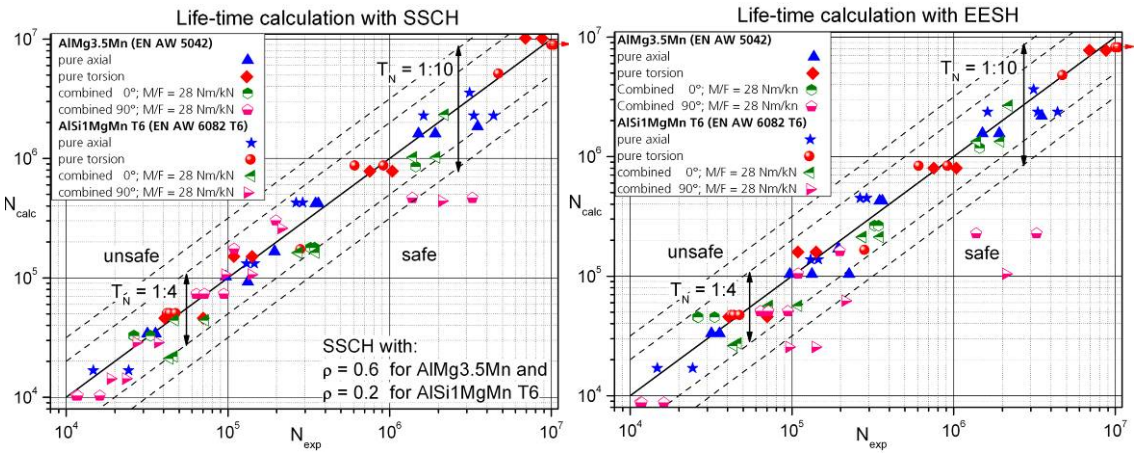

Figure 7. N_{calc} vs. N_{exp} diagrams for aluminium joints

SUMMARY AND CONCLUSIONS

The laserbeam welded steel and aluminium alloys all show a reduction in lifetime under changing principle stress directions (non-proportional loading). The steel alloy shows the strongest shortening effect, not depending on the cycle range. For the self hardened aluminium alloy the shortening effect is stronger than for the artificially hardening alloy, but for both alloys this effect only occurs in a range below $2 \cdot 10^5$ cycles.

In case of non-proportional loadings, a calculation with the von Mises approach would overestimate the lifetimes for all three alloys, because the von Mises equivalent stress is smaller compared to the proportional case. However, calculations with EESH and SSCH lead to a satisfactory estimation that tends more to the safe side than to the unsafe side.

REFERENCES

1. Störzel, K.; Wiebesiek, J.; Bruder, T.; Hanselka (2008) LBF-Bericht Nr. FB-**235**
2. Bruder, T.; Störzel, K.; Baumgartner, J. (2008) Proceedings of the 2nd Symposium on Structural Durability SOSDID, pp. 183 - 197
3. Sonsino, C.M. (1995) Int. J. Fatigue **17**, pp. 55-70
4. Sonsino, C.M., Kueppers, M., Eibl, M., Zhang, G. (2006), Int. J. Fatigue **28**, pp. 657-662
5. Eibl, M., Sonsino, C.M., Kaufmann, H., Zhang, G. (2003) Int. J. Fatigue **25**, pp. 719-731
6. Sonsino, C.M. (2009) Welding in the World **53** ¾, pp. R64-R75

ACKNOWLEDGMENT

The authors thank Professor C.M. Sonsino for supporting these research projects.